Eur. Phys. J. B (2018) 91: 278
https://doi.org/10.1140/epjb/e2018-90266-6

THE EUROPEAN PHYSICAL JOURNAL B

Regular Article

# London penetration depth in the ensemble of spin polarons of cuprate superconductors

Dmitry M. Dzebisashvili[1,2,a] and Konstantin K. Komarov[1]

[1] Kirensky Institute of Physics, Federal Research Center KSC SB RAS, Krasnoyarsk 660036, Russia
[2] Reshetnev Siberian State University of Science and Technology, Krasnoyarsk 660037, Russia

Received 19 April 2018 / Received in final form 19 July 2018
Published online 13 November 2018


**Abstract.** Within the spin-polaron concept for hole-doped cuprates superconductors the temperature and doping dependence of the London penetration depth $\lambda$ is studied. To calculate $\lambda$ we developed a novel approach which (i) does not suppose the analytical expression for the quasiparticle spectrum to be known in advance, and (ii) allows to take into account the strong coupling between a spin localized on the copper ion and a hole residing on the four nearest oxygen ions rigorously. Within this approach the expression for supercurrent density $\vec{j}$ is obtained in the long-wavelength limit for external magnetic field vector potential. It is shown that $\vec{j}$ is mainly due to the spin-polaron quasiparticles rather then bare oxygen holes. Temperature dependence of $\lambda^{-2}$ at various doping is calculated and compared with available experimental data. It is argued that the inflection point revealed experimentally in the temperature behavior of $\lambda^{-2}$ in $La_{1.83}Sr_{0.17}CuO_4$ may be considered as a manifestation of the spin-polaron nature of quasiparticles in cuprates.

## 1 Introduction

The explanation for unusual properties of cuprate high-$T_c$ superconductors (HTSC) is based on the concept of strong electron correlations [1] (SEC), which in particular allows one to understand the emergence of significant coupling between charge and spin degrees of freedom in these materials. It turns out that the spin-polaron approach, accounting for the strong spin-fermion coupling rigorously and considering localized spin subsystem in the quantum spin liquid state, proved to be very successful in describing both the normal (N) and superconducting (SC) properties of the hole-doped cuprate HTSC. Substantially, this approach was developed on the basis of two models, namely, the Kondo-lattice model (see Refs. [2–6]), and spin-fermion model (SFM) (Refs. [7–10]).

The SFM [11–18] follows from the three-band $p$–$d$ model or Emery model [19–23] in the regime of SEC after integrating out the doubly occupied and empty states in the two-hole Hilbert space of each copper ion. Thus, the SFM is the low-energy effective version of the Emery model and is characterized by homopolar states of copper ions. In contrast to the more simple and more popular Hubbard model [24] and $t-J$ model [25], the SFM inherit from Emery model the most important features of electronic structure of cuprates. In particular, it preserves the spatial separation of copper and oxygen sites and accounts for two oxygen ions in the unit cell.

The largest effective interactions in the SFM are (1) $p$–$d$ exchange interaction between spins of holes on the nearest copper and oxygen sites and (2) spin-correlated hoppings, i.e., charge transfer between oxygen ions with a simultaneous flipping of the copper and oxygen spins. Mathematically, these strong spin-charge correlations are accounted for by a multiplicative operator defined as a product of a spin operator on the copper site and a Fermi operator on the neighboring oxygen site. Following the spin-polaron approach, the dynamics of the multiplicative operator should be considered as strictly as possible. The convenient way to achieve this is based on the Zwanzig-Mori projection technique [26–33] or the methods closely related to this technique: the spectral density approach [34] and composite operator method [35–38]. According to the projection technique, one have to include the multiplicative operator into the set of basis operators, write down the equations of motion for the extended set of basis operators, and to project obtained equations onto the same basis. Since within this procedure the multiplicative operator is not decoupled, the short-range spin-fermion correlations will be taken into account rigorously.

Another result of this procedure is that the spectral properties of the system acquire strong dependence on the spin-spin correlation functions. Various techniques were elaborated to determine doping dependence of these spin

[a] e-mail: ddm@iph.krasn.ru

correlators provided that the system is in the quantum spin liquid state [39–45]. The quasiparticles arising within the discussed approach turn out to have all features of the spin polarons whose origin is closely related to the Zhang-Rice singlets [46]. The excitation spectrum and spectral density of these quasiparticles were the subject of intensive research at the early stage of development of the spin-polaron approach [7–10].

Specifically, it was shown that the Fermi surface in the form of a "hole pocket" in the vicinity of the $(\pi/2, \pi/2)$-point of the Brillouin zone, observed in ARPES-experiments [47], is well reproduced. It was found that the important role of direct oxygen-oxygen hoppings is to remove the strong anisotropy of the spin-polaron spectrum around the band minima [48]. In reference [49], the same conclusion was drawn within the SFM but in different approach. To describe the pseudogap (PG) behavior in cuprates, the spin-polaron approach was extended [50,51] by involving the coupling of a local spin polaron with an antiferromagnetic spin wave with momentum $\vec{Q} = (\pi, \pi)$. This approach was also used to investigate the dispersion of the dielectric function in cuprates [52]. Experimentally measured in $La_{2-x}Sr_xCuO_4$ doping evolution of the Fermi momentum [53] was also successfully described within the spin polaron approach [54]. At last, the effects of finite hole density on the spectral properties were investigated [55] by taking into account the spin-fermion correlators.

The spin polaron approach got the second breath when the authors of references [56–58] managed to describe the cooper instability in the ensemble of spin-polaron quasiparticles. First, it was shown that the $d$-wave superconducting dome in the $T-x$ phase diagram is reproduced and agrees well with the experimental one in both the maximal critical temperature $T_c$ and doping range where superconductivity exists. The coupling constant in this case was shown to be the exchange integral describing the intensity of exchange interaction between two localized spins. Shortly after that a very important fact was established. It turns out that the Coulomb interaction between holes on the nearest oxygen ions does not affect the $d$-wave superconductivity in cuprates since the Fourier transform of this interaction falls out of the corresponding self-consistency equations [59,60]. Another substantial result obtained within the approach was that the $s$-wave superconductivity does not occur in the actual doping range since equations for $s$-wave order parameter do not have nontrivial solutions [61].

In the present paper, the next step is taken towards further development of the spin-polaron approach. Specifically, the temperature dependence of the London penetration depth $\lambda$ for cuprate HTSC at various dopings is calculated and compared with experimental data.

For this purpose, we derived at first the expression for current density $\vec{j}(\vec{q} = 0)$ induced by uniform vector potential $\vec{A}_{\vec{q}=0}$ in the ensemble of spin-polaron quasiparticles in the $d$-wave SC state. Then the inverse square of $\lambda$ is found by numerical differentiation of the current density with respect to the vector potential in the limit of small $\vec{A}_{\vec{q}=0}$. This approach differs from the standard ones [62–64] and those adopted for cuprates [65–71] since the latter are aimed to obtain the expression directly for the response function. Unlike the conventional schemes, our approach (1) does not require the analytical expression for quasiparticle spectrum to be known in advance; (2) can be easily generalized to multiband systems; (3) is not limited to very small values of $\vec{A}_{\vec{q}=0}$ when calculating $\vec{j}(\vec{q} = 0)$. The obtained temperature dependencies of $\lambda^{-2}$ are compared to the available experimental data [72–80] and evidence of the spin-polaron nature of quasiparticles in cuprates is found.

The paper is organized as follows. In Section 2, the Hamiltonian of the SFM is formulated. In Section 3 this Hamiltonian is generalized in such a way as to take into account the vector potential of magnetic field in the long wavelength limit. Detailed explanation of our method for deriving the current density within the spin-polaron approach is given in Section 4. In Section 5, the excitation spectrum of spin-polaron quasiparticles in the SC state and in the presence of a vector potential is derived. In Section 6, the expression for $d$-wave order parameter is discussed. Self-consistency equations for the order parameter, chemical potential, and superconducting current density are summarized in Section 7. In Section 8, we present the results of our numerical calculations of the magnetic penetration depth temperature dependencies which are compared with the available experimental data. We conclude the paper with a brief summary in Section 9.

## 2 Hamiltonian of the spin-fermion model

It is known that the main features of electronic structure of the $CuO_2$ plane in the high-$T_c$ cuprate superconductors are well reproduced by the three band $p-d$ model or the Emery model [19–21]. The most essential parameters of the model are (1) the charge transfer gap $\Delta_{pd} = \varepsilon_p - \varepsilon_d$, where $\varepsilon_{p(d)}$ is the energy of a hole on the oxygen (copper) $p(d)$-orbital; (2) the $p-d$ hybridization parameter $t_{pd}$; (3) the Coulomb interaction $U_d$ of two holes on the same copper ion; and (4) the transfer integral $t^{pp}$, describing hopping of holes in the oxygen subsystem. Other parameters of the Emery model, such as Coulomb interaction of two holes on the same ($U_p$) and different ($V_{pp}$) oxygen sites, and interaction of holes on oxygen and copper sites ($V_{pd}$) are left out for simplicity in the present study.

If in the $CuO_2$ plane there is exactly one hole per unit cell then, according to experimental data, the system is in the Mott-Hubbard insulating state. In the Emery model this type of the ground state occurs in the regime of SEC when

$$U_d > \Delta_{pd} \gg t_{pd} > 0. \tag{1}$$

In this regime the Emery model may be reduced to the spin-fermion model [11–18] with the Hamiltonian [8]:

$$\hat{\mathscr{H}} = (\varepsilon_p - \mu) \sum_l p_l^+ p_l + \sum_{ll'} t_{ll'} p_l^+ p_{l'} + \sum_{f\delta\delta_1} \zeta_\delta \zeta_{\delta_1} p_{f+\delta}^+ \left( \frac{\tau}{2} + \frac{J}{4} \tilde{S}_f \right) p_{f+\delta_1} + \hat{\mathscr{H}}_{exch}. \tag{2}$$

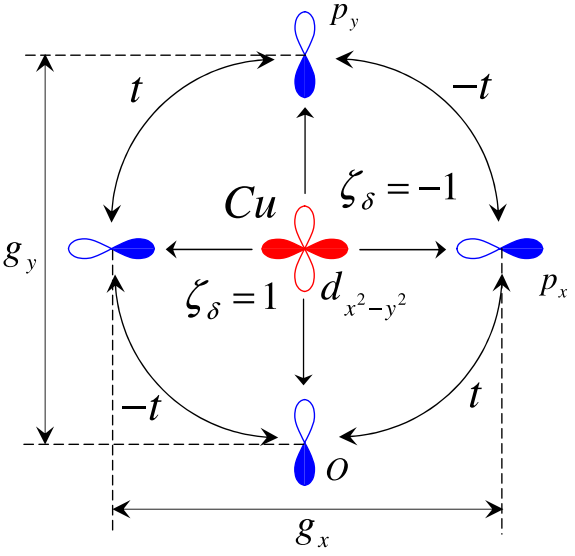


**Fig. 1.** Copper ($d_{x^2-y^2}$) and oxygen ($p_x$, $p_y$) orbitals of holes in the $CuO_2$ plane considered in the Emery model. Shaded parts of the orbitals have positive phase, the open parts of the orbitals correspond to the negative phase. Transfer integral $t$ between different oxygen ions is shown together with its sign which depends on the phases of the corresponding oxygen $p$-orbitals. Vector $\delta$ takes four values $\delta = \{(\pm g_x/2, 0), (0, \pm g_y/2)\}$, connecting copper site with four oxygen sites. Function $\zeta_\delta$ determines the hybridization parameter sign depending on the direction of $\delta$. $g_x$ and $g_y$ are the lattice parameters of the $CuO_2$ plane.

Here, the two-component spinor notations are used for the second quantization operators:

$$p_l^+ = (p_{l\uparrow}^+, p_{l\downarrow}^+), \quad p_l = \begin{pmatrix} p_{l\uparrow} \\ p_{l\downarrow} \end{pmatrix},$$

where operator $p_{l\sigma}^+(p_{l\sigma})$ creates (annihilates) a hole on the oxygen ion with site index $l$, spin projection $\sigma$ ($=\uparrow, \downarrow$), and with the energy $\varepsilon_p$, which is measured from the chemical potential $\mu$. The second term in equation (2) describes hoppings of holes in the oxygen subsystem with $t_{ll'}$ being the tunnelling integral between oxygen sites $l$ and $l'$. The sign of $t_{ll'}$ depends on hopping direction, i.e., $t_{ll'} = +t$ at $l - l' = (\pm g_x/2, \pm g_y/2)$ and $t_{ll'} = -t$ at $l - l' = (\pm g_x/2, \mp g_y/2)$, as is indicated in Figure 1. Here $g_x$ and $g_y$ are the lattice constants along the $x$- and $y$-axes, respectively.

The third term in the effective low-energy Hamiltonian (2) appears in the second order of perturbation theory in the $p$–$d$ hybridization. This term describes both conventional hole hoppings (with tunnelling integral $\tau$ in round brackets) and spin-correlated hoppings (with parameter $J$). In the third sum index $f$ denotes the copper ion position and vectors $\delta$ and $\delta_1$ run independently four vectors connecting copper site $f$ with four nearest oxygen sites (see Fig. 1). The matrix spin operator $\tilde{S}_f$ is defined as a product of a vector spin operator $\vec{S}_f$ and a vector $\vec{\sigma} = (\sigma^x, \sigma^y, \sigma^z)$, compiled from Pauli matrices $\sigma^\alpha$ ($\alpha = x, y, z$):

$$\tilde{S}_f = \vec{S}_f \vec{\sigma} = \begin{pmatrix} S_f^z & S_f^- \\ S_f^+ & -S_f^z \end{pmatrix}.$$

Factors $\zeta_\delta$ in the third sum of equation (2) take into account the sign of hybridization parameter $t_{pd}$ depending on vector $\delta$, i.e., $\zeta_\delta = \mp 1$ for $\delta = \{(\pm g_x/2, 0), (0, \pm g_y/2)\}$.

The connection of parameters $\tau$ and $J$ with that of original Emery model is given by the relations:

$$\tau = \frac{t_{pd}^2}{\Delta_{pd}} \left(1 - \frac{\Delta_{pd}}{U_d - \Delta_{pd}}\right),$$
$$J = \frac{4t_{pd}^2}{\Delta_{pd}} \left(1 + \frac{\Delta_{pd}}{U_d - \Delta_{pd}}\right). \quad (3)$$

In the fourth order of perturbation theory in $p$–$d$ hybridization the exchange interaction between spins on the nearest copper ions arises. The last term in equation (2) refers to this exchange interaction and has the form

$$\hat{\mathscr{H}}_{exch} = \frac{I}{2} \sum_{f\delta} \vec{S}_f \vec{S}_{f+2\delta}, \quad (4)$$

where $I$ is the exchange integral. In the present study the localized spin subsystem is considered in the SU(2)-invariant spin-liquid state. This means that the long-range magnetic order is absent: $\langle S_f^\alpha \rangle = 0$ ($\alpha = x, y, z$), but short-range spin correlations are preserved. To quantify the short-range magnetic order, the two-site spin correlation functions $C_j$ are introduced. These functions are defined as thermodynamic averages

$$C_j = 3\langle S_f^\alpha S_{f+r_j}^\alpha \rangle, \quad \alpha = x, y, z, \quad (5)$$

for two spins located at a distance $r_j$ where $j$ is a number of coordination sphere with respect to the site $f$.

Below, we shall regard the spin correlators $C_j$ as parameters with their values as obtained from calculations for the frustrated Heisenberg spin system on the square lattice within the spherically symmetric approach [44]. The doping dependence of $C_j$ will be modeled by varying the frustration intensity [51]. In the low-temperature region of interest the spin correlators are almost independent of $T$.

The Hamiltonian (2) of the SFM is the starting point of our study. In what follows we adopt the well established Emery model parameters [81,82] (in eV): $t_{pd} = 1.3$, $\Delta_{pd} = 3.6$, $U_d = 10.5$. For the oxygen-oxygen hopping integral we take $t = 0.12$ eV which is a reduced value as compared to the one usually used. For choosing this value of $t$ we have at least two reasons following from our previous study of cuprate HTSC in both N-phase [54] and SC-phase [58]. The exchange constant was chosen to be $I = 0.118$ eV to conform the Neel temperature in undoped cuprates [82].

Using these Emery model parameters the parameters of SFM are easily found from its definition (3): $\tau = 0.225$ eV, $J = 2.86$ eV. It is the large value of

$J$ ($\gg \tau,\ t,\ I$) that allows us to introduce the concept of a spin polaron in cuprates within the SFM model. In the form used here this concept was formulated in reference [8].

## 3 Spin-fermion model with accounting for the vector potential of magnetic field

We intend to obtain the expression for the magnetic penetration depth $\lambda$ using the London equation: $\vec{j} = -c/(4\pi\lambda^2)\vec{A}$, relating the superconducting current density $\vec{j}$ and the vector potential $\vec{A}$ in the local approximation. Hence, the prime task is to calculate the current density in the ensemble of spin polaron quasiparticles. For this purpose we need to incorporate the magnetic field into the Hamiltonian of the SFM (2).

In the tight-binding approximation, used for the SFM formulation, the convenient way to do this is based on the Peierls substitution. Applying the substitution for the tunnelling integral $t_{ll'}$ in the Hamiltonian (2) we have:

$$t_{ll'} \Rightarrow t_{ll'} \exp\left\{\frac{ie}{c\hbar}\int_{R_l'}^{R_l} d\vec{r}\vec{A}(\vec{r})\right\}, \tag{6}$$

where $R_l$ is the radius-vector of the $l$th site, $\hbar$ is the Planck's constant, $e$ is electron charge, and $c$ the speed of light. Since eventually we are interested only in the limit of uniform vector potential (weak magnetic field), we set $\vec{A}(\vec{r}) = \vec{A}_{\vec{q}=0}$ at the very beginning and, to be specific, direct the vector $\vec{A}_{\vec{q}=0}$ along the $x$-axis. In this case, according to (6), the transfer integral $t_{ll'}$ acquires a factor

$$\exp\left\{\frac{ie}{c\hbar}R^x_{ll'}A^x_{q=0}\right\}, \tag{7}$$

where $R_{ll'} = R_l - R_{l'}$. Similarly, the factor

$$\exp\left\{\frac{ie}{c\hbar}(\delta^x - \delta^x_1)A^x_{q=0}\right\}, \tag{8}$$

turns out to be attached to each term in the third sum of the Hamiltonian (2).

The conventional approach [62–71] for derivation of the current density operator is to expand the exponential factors (7) and (8) in the vector potential $A^x_{q=0}$, assuming this to be small. Then, taking into account only the first- and second-order corrections to the Hamiltonian, and by varying these corrections with respect to the vector potential $A^x_{q=0}$, one obtains the paramagnetic and diamagnetic parts of the superconducting current density operator.

Moving away from the conventional approach, first of all for the sake of convenience of calculations, we assume $A^x_{q=0}$ not to be small, and therefore will not expand the factors (7) and (8). At the same time of course we have to keep in mind that the vector potential should not exceed the value above which the Peierls substitution is not valid.

The advantage of keeping exponents (7) and (8) as they are, becomes clear after Fourier transformation

$$p_{f\pm\frac{g_x}{2},\sigma} = N^{-1/2}\sum_k e^{ik(R_f\pm\frac{g_x}{2})}a_{k\sigma},$$
$$p_{f\pm\frac{g_y}{2},\sigma} = N^{-1/2}\sum_k e^{ik(R_f\pm\frac{g_y}{2})}b_{k\sigma}, \tag{9}$$

where $N$ is the number of unit cells in the $CuO_2$ plane. Transformation (9) describes transition to the new second quantization operators $a_{k\sigma}$ and $b_{k\sigma}$. These operators correspond to annihilation of a hole with a quasimomentum $k$ and spin $\sigma$ in the $x$ and $y$ oxygen sublattices, respectively.

After Fourier transform (9), the Hamiltonian (2) takes the form

$$\hat{\mathscr{H}} = \sum_k \left[\xi_{kx}a_k^+a_k + \xi_{ky}b_k^+b_k + \Gamma_k(a_k^+b_k + b_k^+a_k) + Ju_k^+L_k\right] + \hat{\mathscr{H}}_{exch}, \tag{10}$$

where

$$\xi_{kx} = \varepsilon_p - \mu + 2\tau\nu^2_{kx},\quad \xi_{ky} = \varepsilon_p - \mu + 2\tau\nu^2_{ky},$$
$$\Gamma_k = (2\tau - 4t)\nu_{kx}\nu_{ky},\quad u_k = \nu_{kx}a_k + \nu_{ky}b_k,$$
$$L_k = \sum_q \tilde{S}_{k-q}u_q,\quad \tilde{S}_k = \frac{1}{N}\sum_f e^{-ikR_f}\tilde{S}_f,$$
$$\nu_{kx} = \sin\left(\frac{k_x}{2} - \alpha_x\right),\quad \nu_{ky} = \sin\left(\frac{k_y}{2}\right). \tag{11}$$

When writing expression (10), two new operators were introduced: operator $u_k$, which is a superposition of $a_k$ and $b_k$, and operator $L_k$, accounting for the coupling of a localized copper spin and a hole on the four nearest oxygen ions.

A remarkable feature of the resulting Hamiltonian (10) is that the dimensionless vector potential field

$$\alpha_x = \frac{eg_x}{2c\hbar}A^x_{q=0}, \tag{12}$$

enters the Hamiltonian only as a phase shift in the argument of the trigonometric function $\nu_{kx}$. Obviously, if we take into account the $y$-component of the field $\vec{A}$ along with the $x$-component, then a corresponding phase shift would appear in the argument of the function $\nu_{ky}$ as well.

## 4 Superconducting current density and projection method

Varying expression (10) for the Hamiltonian of the SFM with respect to the vector potential $A^x_{q=0}$ and comparing the obtained result with the definition of the current density operator

$$\delta\hat{\mathscr{H}} = -\frac{1}{c}\sum_q \hat{j}_x(-q)\delta A^x_q, \tag{13}$$

we obtain following expression for the supercurrent density mean value $j_x(q) = \langle \hat{j}_x(q) \rangle$ in the long wavelength limit:

$$j_x(q=0) = \frac{eg_x}{\hbar} \sum_k \cos\left(\frac{k_x}{2} - \alpha_x\right) \left[2\tau\nu_{kx}\langle a_k^+ a_k\rangle + (2\tau - 4t)\nu_{ky}\langle a_k^+ b_k\rangle + J\langle a_k^+ L_k\rangle\right]. \quad (14)$$

It should be noted that, according to aforesaid, the expression (14) for the superconducting current density is valid not only at small fields $\alpha_x$.

The thermodynamical averages denoted in (14) by angle brackets have to be calculated using statistical operator with the Hamiltonian (10) accounting for the vector potential $A^x_{q=0}$. Moreover, in computing the averages, the spin polaron nature of quasiparticles should be taken into consideration. As was mentioned above, this can be conveniently done within the spin-polaron approach [8] developed on the basis of the Zwanzig-Mori projection technique [26–29,33].

According to this approach the set of basis operators $B_j$ $(j = 1, \ldots, n)$ is introduced, where $n$ determines the minimal number of basis operators sufficient for describing the spectral and thermodynamical properties of the system under consideration. Then retarded two-time temperature Green's functions (GF) $(i, j = 1, \ldots, n)$:

$$G_{ij}(k, t-t') \equiv \langle\langle B_{ik\sigma}(t)|B^+_{jk\sigma}(t')\rangle\rangle = -i\theta(t-t')\langle[B_{ik\sigma}(t), B^+_{jk\sigma}(t')]\rangle, \quad (15)$$

are defined. In equation (15), the operators $B_{jk\sigma}(t)$ are in the Heisenberg representation and $\theta(t)$ is the Heaviside step function.

The set of $n \times n$ equations of motion for the Fourier transforms of the GFs (15) has the form:

$$\omega\langle\langle B_{ik\sigma}|B^+_{jk\sigma}\rangle\rangle_\omega = K_{ij}(k) + \langle\langle[B_{ik\sigma}, \hat{\mathscr{H}}\,]|B^+_{jk\sigma}\rangle\rangle_\omega, \quad (16)$$

where the terms $K_{ij}(k)$ are determined as averaged anticommutator

$$K_{ij}(k) = \langle\{B_{ik\sigma}, B^+_{jk\sigma}\}\rangle. \quad (17)$$

In accordance with the projection technique, the GFs obtained by commuting the operator $B_{ik\sigma}$ with the Hamiltonian $\hat{\mathscr{H}}$ are represented as a linear superposition of basis GFs (15):

$$\langle\langle[B_{ik\sigma}, \hat{\mathscr{H}}\,]|B^+_{jk\sigma}\rangle\rangle_\omega = \sum_l L_{il}(k)\langle\langle B_{lk\sigma}|B^+_{jk\sigma}\rangle\rangle_\omega. \quad (18)$$

Here, $L_{ij}(k)$ is an $ij$th element of the matrix product $D(k)K^{-1}(k)$, where matrix $D(k)$ is defined by elements

$$D_{ij}(k) = \langle\{[B_{ik\sigma}, \hat{\mathscr{H}}\,], B^+_{jk\sigma}\}\rangle, \quad (19)$$

and the elements of matrix $K(k)$ are given in (17).

Thereafter, the set of equations for the GFs $G_{ij}(k,\omega) = \langle\langle B_{ik\sigma}|B^+_{jk\sigma}\rangle\rangle_\omega$ turns out to be closed and can be solved in the matrix form:

$$G(k,\omega) = M(k,\omega)^{-1}K(k), \quad (20)$$

where $G(k,\omega)$ is the matrix GF and

$$M(k,\omega) = \omega - D(k)K^{-1}(k). \quad (21)$$

The energy spectrum of quasiparticles is determined by the poles of the GF and can be obtained from the dispersion equation:

$$\det M(k,\omega) = 0. \quad (22)$$

As was shown in reference [51], to describe correctly the N-phase spectral properties of cuprates, besides operators $a_k$ and $b_k$, it is necessary to include into the basis set the third operator $L_k$ (11). It is this operator that allows us to describe the strong coupling between a localized spin and a hole on the nearest oxygen ions properly. Thus, the minimal operator basis should consist of three operators:

$$B_{1k} = a_{k\uparrow}, \quad B_{2k} = b_{k\uparrow}, \quad B_{3k} = L_{k\uparrow}. \quad (23)$$

According to definition (19) in order to derive matrix element $D_{ij}(k)$ one needs to calculate commutator of the $i's$ basis operator with the Hamiltonian $\hat{\mathscr{H}}$ and then anticommute the result with the $j's$ basis operator. Doing so one obtains in general rather complicated correlation functions, involving spin and fermion operators, and which has to be approximated somehow. Hereafter, we adopt the low-density approximation which means that all normal (i.e., non-anomalous) correlation functions arising in calculation $D_{ij}(k)$ and involving fermion operators are neglected as compared to the purely spin correlators. This approximation is justified by the low hole doping which in cuprates of interest does not exceed the value of $x \cong 0.22$ so that all spin-fermion correlators are several times smaller then the spin-spin correlators.

Thus, calculating the matrix elements (19) of the symmetric $3 \times 3$ matrix $D^{(3)}(k)$ using basis (23) in the low-density limit we obtain (see Appendix):

$$\begin{aligned} &D_{11}(k) = \xi_{kx}, \quad D_{22}(k) = \xi_{ky}, \quad D_{12}(k) = \Gamma_k, \\ &D_{13}(k) = J\nu_{kx}K_k, \quad D_{23}(k) = J\nu_{ky}K_k, \\ &D_{33}(k) = (\varepsilon_p - \mu + 4\tau - 4t)K_k - \frac{9}{8}\tau + \frac{3}{2}t \\ &\qquad + (\tau - 2t)C_2\gamma_{2k} + \frac{1}{2}\tau C_3\gamma_{3k} - \frac{3}{4}J \\ &\qquad + JC_1(1/4 + 2\gamma_{1k}) - IC_1(\gamma_{1k} + 4), \end{aligned} \quad (24)$$

where

$$K_k = \frac{3}{4} - C_1\gamma_{1k} \quad (25)$$

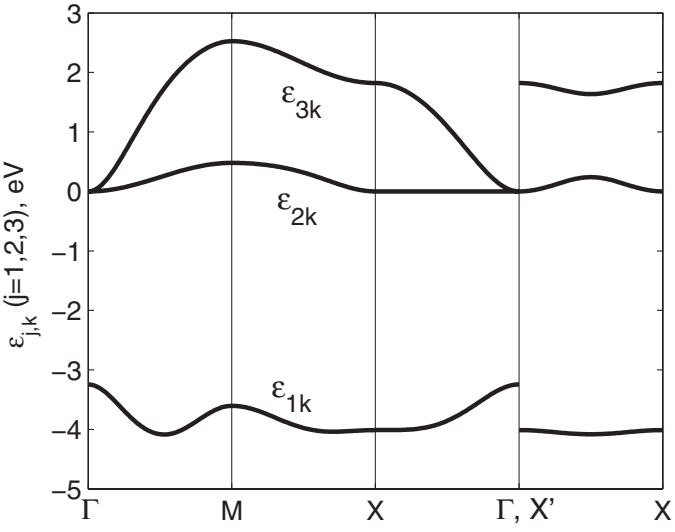


**Fig. 2.** Fermi excitations spectrum of the SFM in the N-phase. Three branches of the spectrum $\varepsilon_{jk}$ $(j = 1, 2, 3)$ are the solutions of the dispersion equation (29). The lower band corresponds to the spin-polaron states formed due to the strong spin-fermion coupling. The vector potential for simplicity is taken to be zero since for any reasonable value of $A^x_{q=0}$ the curves differ insignificantly in the scale of the bandwidth. The notations for the symmetry points of the Brillouin zone are as follows: $\Gamma = (0, 0)$, $M = (\pi, \pi)$, $X = (0, \pi)$, $X' = (\pi, 0)$ (in units of lattice spacing).

is one of the elements of the diagonal matrix

$$K^{(3)}(k) = \mathrm{diag}\{1, 1, K_k\}, \tag{26}$$

and functions $\gamma_{jk}$ $(j = 1, 2, 3)$ are defined as

$$\begin{aligned}\gamma_{1k} &= (\cos(k_x - 2\alpha_x) + \cos k_y)/2,\\ \gamma_{2k} &= \cos(k_x - 2\alpha_x)\cos k_y,\\ \gamma_{3k} &= (\cos(2k_x - 4\alpha_x) + \cos 2k_y)/2.\end{aligned} \tag{27}$$

Besides, in calculating matrix elements (24) and (25) there appeared the spin correlators $C_j$ $(j = 1, 2, 3)$ which were introduced in (5).

The $3 \times 3$ matrix $M(k, \omega)$ (21), denoted further as $M^{(3)}(k, \omega)$, reads

$$M^{(3)}(k,\omega) = \begin{pmatrix} \omega - D_{11}(k) & -D_{12}(k) & -\frac{D_{13}(k)}{K_k} \\ -D_{12}(k) & \omega - D_{22}(k) & -\frac{D_{23}(k)}{K_k} \\ -D_{13}(k) & -D_{23}(k) & \omega - \frac{D_{33}(k)}{K_k} \end{pmatrix}. \tag{28}$$

Fermi spectrum of the spin-polaron quasiparticles in the N-phase follows from the dispersion equation

$$\det M^{(3)}(k, \omega) = 0, \tag{29}$$

and corresponds to the lower branch $\varepsilon_{1k}$ in Figure 2. For simplicity the band structure depicted in Figure 2 is calculated at $A^x_{q=0} = 0$ since at any finite but reasonable value of the vector potential these dispersion curves differ insignificantly on the scale of the bandwidth. An important feature of the spectrum $\varepsilon_{1k}$ is that the band minimum is located in the vicinity of the $(\pi/2, \pi/2)$ point of the Brillouin zone. It is this minimum that gives rise to a small hole pockets [8,51,54] observed in ARPES-experiments [47] at low doping. Another important feature of the spin-polaron band is that it is splitted down from the upper bands by a large energy gap order of $J$. Obviously, the considerable energy gain of these spin-polaron states is due to the strong coupling of a localized copper spin and a hole on the four nearest oxygen ions.

Before discussing superconducting properties of cuprates within the spin-polaron approach let us first show that the current density (14) calculated in N-phase must be zero identically. In conventional approaches the zero value of the net current in N-phase is provided by cancellation of the paramagnetic and diamagnetic current density parts. In the developed here approach we do not distinguish paramagnetic and diamagnetic parts of the current density and hence zero value of the net current must be achieved by another way.

According to the expression (14) to calculate the current density we have to know three thermodynamical averages: $\langle a^+_{k\uparrow} a_{k\uparrow}\rangle$, $\langle a^+_{k\uparrow} b_{k\uparrow}\rangle$, and $\langle a^+_{k\uparrow} L_{k\uparrow}\rangle$. These averages can be easily found by using the spectral theorem for the corresponding three GFs. Solving the set of equations (20) with matrices $K^{(3)}(k)$ (26) and $M^{(3)}(k, \omega)$ (28), we obtain the three required GFs in the N-phase:

$$\begin{aligned}\langle\langle a_{k\uparrow}|a^+_{k\uparrow}\rangle\rangle_\omega &= \frac{Q_{11}(k,\omega)}{\det M^{(3)}(k,\omega)},\\ \langle\langle b_{k\uparrow}|a^+_{k\uparrow}\rangle\rangle_\omega &= \frac{-Q_{12}(k,\omega)}{\det M^{(3)}(k,\omega)},\\ \langle\langle L_{k\uparrow}|a^+_{k\uparrow}\rangle\rangle_\omega &= \frac{Q_{13}(k,\omega)}{\det M^{(3)}(k,\omega)},\end{aligned} \tag{30}$$

where $Q_{ij}(k, \omega)$ is a minor to the $ij$th element of the matrix $M^{(3)}(k, \omega)$ (28):

$$\begin{aligned}Q_{11}(k,\omega) &= (\omega - D_{22}(k))(\omega - D_{33}(k)/K_k)\\ &\quad - (D_{23}(k))^2/K_k,\\ Q_{12}(k,\omega) &= -D_{12}(k)(\omega - D_{33}(k)/K_k)\\ &\quad - D_{13}(k)D_{23}(k)/K_k,\\ Q_{13}(k,\omega) &= D_{13}(k)(\omega - D_{22}(k))\\ &\quad + D_{12}(k)D_{23}(k).\end{aligned} \tag{31}$$

The resulting expression for the current density in the N-state is

$$\begin{aligned}j_x(q=0) = \frac{2eg_x}{\hbar}\sum_k \cos\left(\frac{k_x}{2} - \alpha_x\right)\\ \times \frac{f(\varepsilon_{1k}/T)}{(\varepsilon_{1k} - \varepsilon_{2k})(\varepsilon_{1k} - \varepsilon_{3k})}\left[2\tau\nu_{kx}Q_{11}(k,\varepsilon_{1k})\right.\\ \left. -(2\tau - 4t)\nu_{ky}Q_{12}(k,\varepsilon_{1k}) + JQ_{13}(k,\varepsilon_{1k})\right],\end{aligned} \tag{32}$$

where $f(x) = (e^x + 1)^{-1}$ is a Fermi-Dirac distribution function and $\varepsilon_{jk}$ $(j = 1, 2, 3)$ are solutions of the dispersion equation (29) which determines three branches of the Fermi excitation spectrum in the N-phase and in the field of the vector potential. When writing (32), we also took into account that in the considered low-density regime the chemical potential $\mu$ is in the lower spin-polaron band, so that the upper two bands are empty.

It is clear from the expression (32) that dependence of the integrand on the dimensionless vector potential $\alpha_x$ comes out only as a shift of the $x$-component of the quasimomentum $\vec{k}$. Since the integration in (32) is over first Brillouin zone, which also determines the periodicity of the integrand, it is obvious that shifting the integration variable $k_x$ by the value of $\alpha_x$, we can get rid of $\alpha_x$ completely. After that, the integrand function turns out to be antisymmetric with respect to the quasimomentum $\vec{k}$ and, as a consequence, the current density $j_x(q = 0)$ vanishes identically as it should be in the N-phase.

## 5 Spin-polaron spectrum in the superconducting phase with accounting for the vector potential

To study the SC-phase of cuprates, the three-operator basis (23) is not sufficient. In this case, as shown in reference [56], the basis (23) should be extended by additional three operators:

$$B_{4k} = a^+_{-k\downarrow}, \quad B_{5k} = b^+_{-k\downarrow}, \quad B_{6k} = L^+_{-k\downarrow}. \tag{33}$$

Hence, now we need three $6 \times 6$ matrices $K^{(6)}(k)$, $D^{(6)}(k)$, and $M^{(6)}(k, \omega)$ defined by equations (17), (19) and (21), respectively.

As before, the matrix $K^{(6)}(k)$ is diagonal

$$K^{(6)}(k) = \mathrm{diag}\{1, 1, K_k, 1, 1, K_{-k}\}. \tag{34}$$

Note that $K_{-k} \neq K_k$ if $\alpha_x \neq 0$.

The normal components of the energy matrix $D^{(6)}_{ij}(k)$ with indices $i, j = 1, 2, 3$ were calculated earlier and are given in (24). The normal components with indices $i, j = 4, 5, 6$ turn out to be related to that given in (24) by equations:

$$D^{(6)}_{i+3,j+3}(k) = -D^{(6)}_{ij}(-k), \quad i, j = 1, 2, 3. \tag{35}$$

Among the anomalous components of the energy matrix only two of them, $D^{(6)}_{36}(k)$ and $D^{(6)}_{63}(k) = \left(D^{(6)}_{36}(k)\right)^*$, are not equal to zero. The calculations show (see Appendix) that for the superconducting $d$-wave pairing, relevant for cuprates, the anomalous component can be written as follows [56]:

$$D^{(6)}_{36}(k) = \frac{1}{N}\sum_q I_{k+q}\left[\langle L_{q\uparrow} L_{-q\downarrow}\rangle - C_1\langle u_{q\uparrow} u_{-q\downarrow}\rangle\right], \tag{36}$$

where

$$I_k = 2I(\cos k_x + \cos k_y) \tag{37}$$

is a Fourier transform of the exchange integral. Note that, unlike to what we had before, in the expression (37) there is no phase shift of $k_x$ due to the vector potential $\alpha_x$.

It is convenient to express matrix $M^{(6)}(k, \omega)$ in the block form

$$M^{(6)}(k, \omega) = \begin{pmatrix} M^{(3)}(k, \omega) & F^{(3)}(k, \omega) \\ \left(F^{(3)}(k, \omega)\right)^* & \bar{M}^{(3)}(k, \omega) \end{pmatrix}. \tag{38}$$

The upper left $3 \times 3$ block $M^{(3)}(k, \omega)$ is defined in (28). The lower right block $\bar{M}^{(3)}(k, \omega)$ is obtained from the upper left $M^{(3)}(k, \omega)$ by replacing elements $D_{ij}(k)$ with $-D_{ij}(-k)$. The only non-zero element in the anomalous block $F^{(3)}(k, \omega)$ is $F^{(3)}_{33}(k, \omega)$ and is equal to $-D^{(6)}_{36}(k)$.

The Fermi excitation spectrum of cuprates in the SC-phase is determined by zeros of the determinant $\det M^{(6)}(k, \omega)$. This determinant can be expressed via the third-order determinants:

$$\det M^{(6)}(k, \omega) = \det M^{(3)}(k, \omega) \cdot \det \bar{M}^{(3)}(k, \omega) - Q_{33}(k, \omega)\bar{Q}_{33}(k, \omega)\frac{|D^{(6)}_{36}(k)|^2}{K_k K_{-k}}, \tag{39}$$

where

$$Q_{33}(k, \omega) = (\omega - D_{11}(k))(\omega - D_{22}(k)) - (D_{12}(k))^2$$

and

$$\bar{Q}_{33}(k, \omega) = (\omega + D_{11}(-k))(\omega + D_{22}(-k)) - (D_{12}(-k))^2$$

are minors of the 33rd element of the matrices $M^{(3)}(k, \omega)$ and $\bar{M}^{(3)}(k, \omega)$, respectively.

In the low-density regime when the chemical potential $\mu$ lies in the lower spin-polaron band, separated from the upper two bands by a large energy gap $\sim J$ (see Fig. 2), the spin-polaron spectrum $E_{1k}$ in the SC-phase and with accounting for the vector potential $A^x_{q=0}$ can be found with a high accuracy analytically.

To show this, let us write down the determinant $\det M^{(6)}(k, \omega)$ in two equivalent forms:

$$\prod_{j=1}^{6}(\omega - \varepsilon_{jk}) - Q_{33}(k, \omega)\bar{Q}_{33}(k, \omega)\frac{|D^{(6)}_{36}(k)|^2}{K_k K_{-k}}, \tag{40}$$

and

$$\prod_{j=1}^{6}(\omega - E_{jk}). \tag{41}$$

In equation (40) the functions $\varepsilon_{jk}$ with $j = 1, 2, 3$ and $\varepsilon_{jk}$ with $j = 4, 5, 6$ are solutions of the third order dispersion equations $\det M^{(3)}(k, \omega) = 0$, and $\det \bar{M}^{(3)}(k, \omega) = 0$,

respectively. Between these solutions there are obvious relations: $\varepsilon_{j+3,k} = -\varepsilon_{j,-k}$ $(j = 1, 2, 3)$. Functions $E_{jk}$ $(j = 1, \ldots, 6)$, emerging in (41), are the solutions for the sixth order dispersion equation $\det M^{(6)}(k, \omega) = 0$ and thus represent six branches of the Fermi excitations spectrum of cuprates in the SC-phase with accounting for the vector potential $A^x_{q=0}$.

Since the energy spacing between the chemical potential $\mu$ and the upper bands is large, as compared to the amplitude of the anomalous component $D^{(6)}_{36}(k)$, the dispersion of the upper two bands is not actually modified with the onset of superconductivity. This means that with high accuracy we have $E_{jk} = \varepsilon_{jk}$ for $j = 2, 3, 5, 6$. Hence, the unknown remain the spectrum $E_{1k}$ and its conjugate $E_{4k}$ which in fact is equal to $-E_{1,-k}$.

As far as expressions (40) and (41) are equal to each other identically, we may equate their coefficients for the fifth and fourth powers of $\omega$ and obtain the set of two equations

$$E_{1k} + E_{4k} = \varepsilon_{1k} + \varepsilon_{4k},$$
$$E_{1k}E_{4k} = \varepsilon_{1k}\varepsilon_{4k} - \frac{|D^{(6)}_{36}(k)|^2}{K_k K_{-k}}. \quad (42)$$

The solutions of this set with respect to $E_{1,k}$ and $E_{4,k}$ are

$$E_{1(4)k} = \frac{\varepsilon_{1k} - \varepsilon_{1,-k}}{2} \pm E_k,$$
$$E_k = \sqrt{\left(\frac{\varepsilon_{1k} + \varepsilon_{1,-k}}{2}\right)^2 + \frac{|D^{(6)}_{36}(k)|^2}{K_k K_{-k}}}, \quad (43)$$

where the equality $\varepsilon_{4k} = -\varepsilon_{1,-k}$ was used. It is remarkable that despite the three-band character of the system the Fermi excitation spectrum of spin polarons in the SC-phase is expressed only via the $\varepsilon_{1k}$ - the N-phase spectrum of the same spin-polaron band. The upper branches of the N-phase spectrum, $\varepsilon_{2k}$ and $\varepsilon_{3k}$, do not appear in equation (43).

It should also be stressed that obtained equation (43) for the spin-polaron spectrum in the SC-phase is valid in the presence of the vector potential $A^x_{q=0}$ which so far was not supposed to be small. However, for small values of $\alpha_x$ we can use expansion: $\varepsilon_{jk} = \varepsilon^{(0)}_{jk} + \delta\varepsilon_{jk}$ $(j = 1, 2, 3)$, where $\varepsilon^{(0)}_{jk}$ is the spectrum $\varepsilon_{jk}$ at $\alpha_x = 0$, and $\delta\varepsilon_{jk}$ is a linear in $\alpha_x$ correction to $\varepsilon^{(0)}_{jk}$. It turns out that correction $\delta\varepsilon_{1k}$ is odd in $k$. Taking also into account that corrections to the gap function in (43) are quadratic in $\alpha_x$ (see next section) it follows from (43) that in the linear in $\alpha_x$ approximation the spin-polaron spectra $E_{1k}$ and $E_{4k}$ are shifted by the same value of $\delta\varepsilon_{1k}$:

$$E_{1k} = \delta\varepsilon_{1k} + E^{(0)}_k, \quad E_{4k} = \delta\varepsilon_{1k} - E^{(0)}_k, \quad (44)$$

where

$$E^{(0)}_k = \sqrt{\left(\varepsilon^{(0)}_{1k}\right)^2 + \frac{|D^{(6)}_{36}(k)|^2}{K^2_k}}, \quad (45)$$

and the gap function is taken at $\alpha_x = 0$. It is seen that for small $\alpha_x$ the spectrum of the Bogolyubov quasiparticles is renormalized in the same additive manner as in the conventional theory of the London penetration depth [62,63]. At the same time, the particular quasimomentum dependence of the N-phase spectrum $\varepsilon^{(0)}_{1k}$ (and hence its field-induced correction $\delta\varepsilon_{1k}$) differs substantially from the simplest case of quadratic dispersion, and is defined by the structure of the $CuO_2$ plane and by the strong spin-fermion interactions.

## 6 *d*-wave order parameter

For $d$-wave superconductivity, which is the case for cuprates, the order parameter is the anomalous component of the energy matrix $D^{(6)}_{36}(k)$, determined in equation (36). The anomalous averages entering this equation can be expressed in terms of anomalous GFs: $\langle\langle L_{k\uparrow}|L_{-k\downarrow}\rangle\rangle_\omega$ and $\langle\langle u_{k\uparrow}|u_{-k\downarrow}\rangle\rangle_\omega$. Solving equation (20) with matrices (34) and (38) we find these GFs:

$$\langle\langle L_{k\uparrow}|L_{-k\downarrow}\rangle\rangle_\omega = \frac{Q_{LL}(k,\omega)D^{(6)}_{36}(k)}{\det M^{(6)}(k,\omega)},$$
$$\langle\langle u_{k\uparrow}|u_{-k\downarrow}\rangle\rangle_\omega = \frac{Q_{uu}(k,\omega)D^{(6)}_{36}(k)}{\det M^{(6)}(k,\omega)}, \quad (46)$$

where

$$Q_{LL}(k,\omega) = Q_{33}(k,\omega)\bar{Q}_{33}(k,\omega),$$
$$Q_{uu}(k,\omega) = (\nu_{kx}Q_{13}(k,\omega) - \nu_{ky}Q_{23}(k,\omega))$$
$$\times \left(\nu_{-k,x}\bar{Q}_{13}(k,\omega) - \nu_{-k,y}\bar{Q}_{23}(k,\omega)\right)/K_k K_{-k}. \quad (47)$$

Since the kernel of the integral equation (36) is separable it is obvious that the $d$-wave solution of (36) should have the form

$$D^{(6)}_{36}(k) = \Delta_x \cos k_x - \Delta_y \cos k_y, \quad (48)$$

where in general $\Delta_x$ is not equal to $\Delta_y$. This is because so far (except for the end of the previous section) we considered vector potential $\alpha_x$ to be not small.

In principle, we can find the amplitudes $\Delta_x$ and $\Delta_y$ by solving a set of two equations, following from (36), (46), and (48). However, for the sake of simplicity, we will use the fact that ultimately we are interested in the limit of small values of $\alpha_x$. Numerical estimates show that in this regime the changes of amplitudes $\Delta_x$ and $\Delta_y$ are proportional to the second power of $\alpha_x$. This means that in the linear in $\alpha_x$ approximation we can make no difference between $\Delta_x$ and $\Delta_y$ and, denoting further both of them as $\Delta_0$, for the $d$-wave order parameter we obtain

$$D^{(6)}_{36}(k) = \Delta_0(\cos k_x - \cos k_y). \quad (49)$$

It is interesting to note that even at $\alpha_x = 0$ the $k$-dependence of the gap function on the Fermi contour for

$d$-wave order parameter (49) is described not just by the difference of cosines, but is renormalized by the factor $1/K_k^2$, as it follows from (45).

## 7 Self-consistency equations

Given the foregoing, equation (36) for the amplitude $\Delta_0$ of the superconducting $d$-wave order parameter can be written in the form

$$1 = \frac{\tilde{I}}{N}\sum_k \sum_{j=1,4} \frac{f(-E_{jk}/T)\,(\cos k_x - \cos k_y)^2}{(E_{jk}-\varepsilon_{2k})(E_{jk}-\varepsilon_{3k})} \times \frac{Q_{LL}(k,E_{jk}) - C_1 Q_{uu}(k,E_{jk})}{(-1)^{j+1}2E_k(E_{jk}+\varepsilon_{2,-k})(E_{jk}+\varepsilon_{3,-k})}, \quad (50)$$

where as before $f(x)$ is the Fermi-Dirac distribution function. Besides, in order to mimic the effective changes of the exchange integral $I$ with doping, according to [51] we replaced the integral $I$ by $\tilde{I} = I(1-p)$, where $p$ is the frustration parameter, varying from 0.15 to 0.275 with increasing $x$ from 0.03 to 0.22.

Note again that only the lower spin-polaron band with $j = 1$ (and its conjugate with $j = 4$) is modified with the onset of Cooper instability (equation (43)). The upper branches of the Fermi excitations spectrum with $j = 2$ and 3 remain the same as in the N-state and are defined by the dispersion equation (29).

At a given number $x$ of holes per unit cell equation (50) should be solved together with the equation for the chemical potential $\mu$: $x = \frac{1}{N}\sum_k \left(\langle a_k^+ a_k\rangle + \langle b_k^+ b_k\rangle\right)$. Two GFs required to calculate averages $\langle a_k^+ a_k\rangle$ and $\langle b_k^+ b_k\rangle$ come out as solutions of the matrix equation (20) in the SC phase. Doing the same way as in derivation (46) we find

$$\langle\langle a_{k\sigma}|a_{k\sigma}^+\rangle\rangle_\omega = \frac{Q_{aa}(k,\omega)}{\det M^{(6)}(k,\omega)},$$
$$\langle\langle b_{k\sigma}|b_{k\sigma}^+\rangle\rangle_\omega = \frac{Q_{bb}(k,\omega)}{\det M^{(6)}(k,\omega)}, \quad (51)$$

where

$$Q_{aa[bb]}(k,\omega) = Q_{11[22]}(k,\omega)\det \bar{M}^{(3)}(k,\omega) - (\omega - D_{22[11]}(k))\bar{Q}_{33}(k,\omega) \times |D_{36}^{(6)}(k)|^2 / K_k K_{-k}. \quad (52)$$

After using the spectral theorem for the GFs (51), the equation for the chemical potential takes the form

$$x = \frac{2}{N}\sum_k \sum_{j=1,4} \frac{f(E_{jk}/T)}{(E_{jk}-\varepsilon_{2k})(E_{jk}-\varepsilon_{3k})} \times \frac{Q_{aa}(k,E_{jk}) + Q_{bb}(k,E_{jk})}{(-1)^{j+1}2E_k(E_{jk}+\varepsilon_{2,-k})(E_{jk}+\varepsilon_{3,-k})}. \quad (53)$$

Having the solutions of equations (50) and (53) for $\Delta_0$ and $\mu$, respectively, the supercurrent density can be easily found from (14). Two extra GFs $\langle\langle b_{k\sigma}|a_{k\sigma}^+\rangle\rangle_\omega$ and $\langle\langle L_{k\sigma}|a_{k\sigma}^+\rangle\rangle_\omega$, needed to calculate averages $\langle a_{k\sigma}^+ b_{k\sigma}\rangle$ and $\langle a_{k\sigma}^+ L_{k\sigma}\rangle$ entering equation (14), can be derived as before from the matrix equation (20). The answer is

$$\langle\langle b_{k\sigma}|a_{k\sigma}^+\rangle\rangle_\omega = \frac{Q_{ba}(k,\omega)}{\det M^{(6)}(k,\omega)},$$
$$\langle\langle L_{k\sigma}|a_{k\sigma}^+\rangle\rangle_\omega = \frac{Q_{La}(k,\omega)}{\det M^{(6)}(k,\omega)}, \quad (54)$$

where

$$Q_{ba}(k,\omega) = -Q_{12}(k,\omega)\det \bar{M}^{(3)}(k,\omega) - D_{12}(k)\bar{Q}_{33}(k,\omega)|D_{36}^{(6)}(k)|^2/K_k K_{-k},$$
$$Q_{La}(k,\omega) = Q_{13}(k,\omega)\det \bar{M}^{(3)}(k,\omega). \quad (55)$$

Finally, the expression for the current density is obtained in the form:

$$j_x(q=0) = \frac{2eg_x}{\hbar}\sum_k \sum_{j=1,4} \frac{f(E_{jk}/T)\cos(k_x/2-\alpha_x)}{(E_{jk}-\varepsilon_{2k})(E_{jk}-\varepsilon_{3k})} \times \frac{\Psi(k,E_{jk})}{(-1)^{j+1}2E_k(E_{jk}+\varepsilon_{2,-k})(E_{jk}+\varepsilon_{3,-k})}, \quad (56)$$

where

$$\Psi(k,\omega) = 2\tau\nu_{kx}Q_{aa}(k,\omega) - (2\tau - 4t)\nu_{ky}Q_{ba}(k,\omega) + JQ_{La}(k,\omega). \quad (57)$$

It should be noted once again that when deriving self-consistency equations (50), (53), and (56) we did not assume the vector potential $A_{q=0}^x$ to be small. The only requirement was the smallness of the magnetic field which is the curl of the vector potential. As a consequence, the expression (56) for the supercurrent density do not distinguish the paramagnetic and diamagnetic parts.

In the next section, equations (50), (53), and (56) are used to analyze temperature and concentration dependence of the magnetic penetration depth in cuprates.

## 8 London penetration depth: results and discussion

Now since we are going to calculate magnetic penetration depth using London equation $\vec{j} = -c/(4\pi\lambda^2)\vec{A}$ we have to consider regime of small $A_{q=0}^x$. Then $1/\lambda^2$ will be a linear coefficient in the expansion of the current density (56) with respect to the vector potential. From the computational point of view, it is convenient to determine this coefficient numerically as a ratio $j_x(q=0)/\alpha_x$ taken in the limit of reasonably small $\alpha_x$.

Thus, accounting for the dimensional constants we have an expression for the inverse square of the in-plane

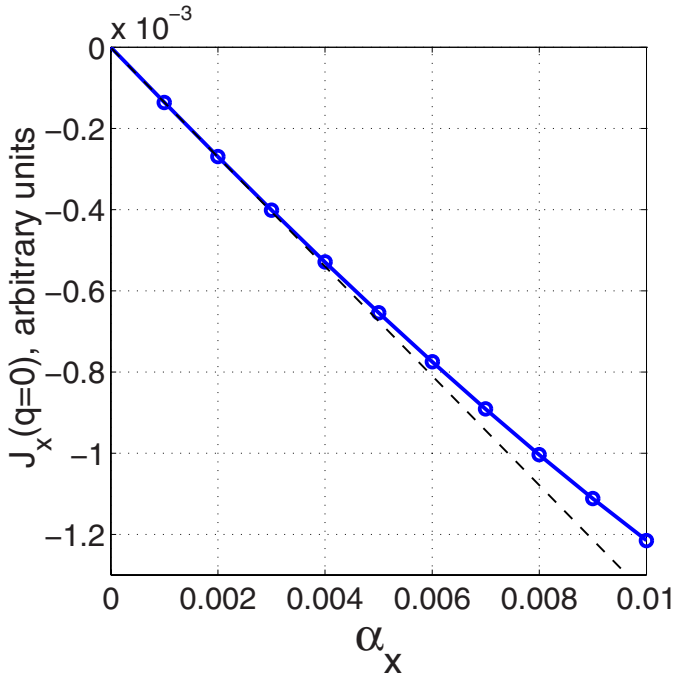


**Fig. 3.** Dependence of the current density $j_x(q=0)$ on the dimensionless vector potential $\alpha_x$. Parameters of the model are as follows (in eV): $\tau = 0.225$, $J = 2.86$, $I = 0.118$, $t = 0.12$. The temperature was taken to be equal 10 K and doping $x = 0.15$. The dashed line is a tangent line at $\alpha_x = 0$.

magnetic penetration depth $\lambda$:

$$\frac{1}{\lambda^2} = -\frac{e\pi}{c^2\hbar\, g_y g_z} \cdot \frac{j_x(q=0)}{N\alpha_x}, \tag{58}$$

where $g_z$ is a lattice spacing along $z$-axis, the supercurrent density $j_x(q=0)$ is defined by equation (56), and the magnitude of the dimensionless vector potential $\alpha_x$ should be taken in the range where the current density depends linearly on $\alpha_x$. The latter condition must be satisfied in order for the penetration depth $\lambda$ have been calculated correctly according to equation (58).

Figure 3 demonstrates the current density calculated self-consistently as a function of $\alpha_x$. It is seen that $j_x(q=0)$ behaves linearly on the interval of $\alpha_x$ from 0 to 0.004. Below we shall use the value $\alpha_x = 0.002$ as most optimal.

The temperature dependencies of the inverse square of the London penetration depth, calculated self-consistently on the basis of equations (50), (53), (56), and (58), at five doping levels: $x = 0.10$, 0.15, 0.20, 0.22, and 0.24, are presented in Figure 4. The parameters of the model were intentionally taken equal to those used in our previous studies of the spectral properties of cuprates [54,55] and its $T_c{-}x$ phase diagram [56–61]. Though we did not adjust the parameters, the obtained value of $\lambda^{-2}(T=0)$ turned out to be within 30% agreement with the experimental data [72–80].

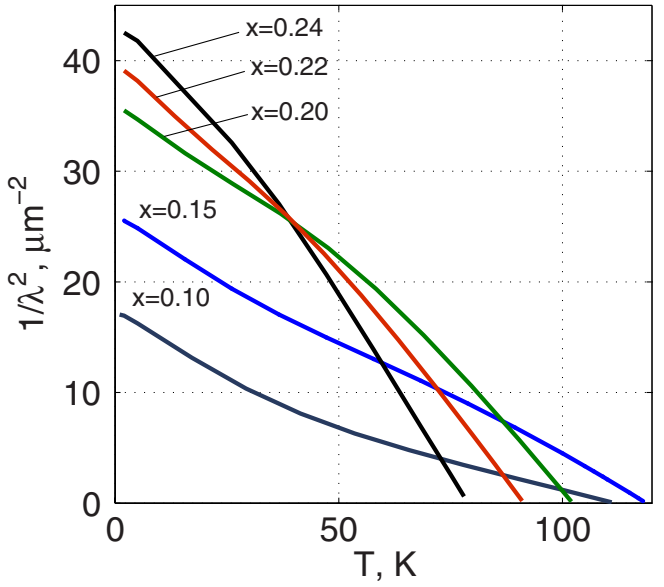


**Fig. 4.** Temperature dependence of the inverse square of the magnetic field penetration depth at five doping levels. The magnitudes of doping $x$ are indicated next to corresponding curves. The model parameters are the same as in Figure 3.

As expected, all the $T$-dependencies of $\lambda^{-2}$ in Figure 4 demonstrate a monotonic decrease from its maximum value at $T = 0$ to zero value at $T = T_c$. The boundary points of these curves, which are the values of $T_c$ and $\lambda^{-2}(T=0)$, can be easily tuned by varying the model parameters. The critical temperature $T_c$, as can be seen from equation (50), is governed by the exchange integral $I$ which measures the strength the holes bind into the Cooper pairs. The value of $\lambda^{-2}$ at $T = 0$ is regulated by the $p{-}d$ exchange parameter $J$. This follows from equations (56–58), and the numerical fact that almost entire contribution to the current density is only due to the third term (proportional to $J$) in equation (57).

Reducing, for instance, superexchange integral down to $I = 0.06$ eV the $T_c{-}x$ phase diagram shrinks considerably as compared to the one calculated for initial model parameters (Fig. 5). As a result, the obtained phase diagram (dashed line in Fig. 5) matches to that of LSCO-superconductors in both the doping interval, limiting the SC dome from $x_1 = 0.05$ up to $x_2 = 0.26$, and the maximum critical temperature $T_{max} = 39$ K. If we simultaneously reduce both $I$ and $J$ by approximately half, then the values of $T_c$ and $\lambda^{-2}(T=0)$ relevant for LSCO (see for example Ref. [75]) are reproduced (Fig. 6). To avoid confusion it is worth noting that the values of both $I = 0.056$ eV and $J = 1.42$ eV (used to calculate the curve in Fig. 6) are underestimated as compared to that generally accepted for cuprates. These values for $I$ and $J$ were used here just to demonstrate (i) the dependence of the maximum value of the $\lambda^{-2}(T=0)$ on $J$, (ii) the dependence of the maximum value of $T_c$ on $I$; and (iii) that experimentally estimated values of $\lambda^{-2}(T=0)$ and $T_c$ for LSCO could be reached by tuning the $p{-}d$ exchange parameter $J$ and the superexchange integral $I$.

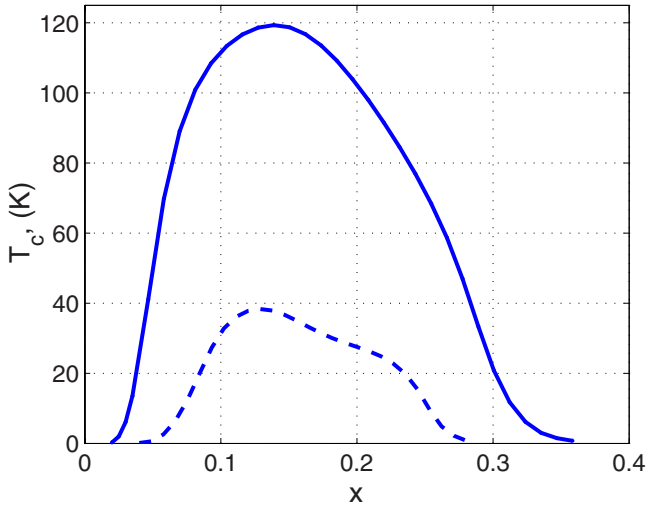


**Fig. 5.** Doping dependence of the critical temperature for two values of the exchange integral: solid line is calculated for $I = 0.118$ eV, dashed line corresponds to $I = 0.06$ eV. The rest of the model parameters are the same as in Figure 3. The vector potential $A^x_{q=0} = 0$.

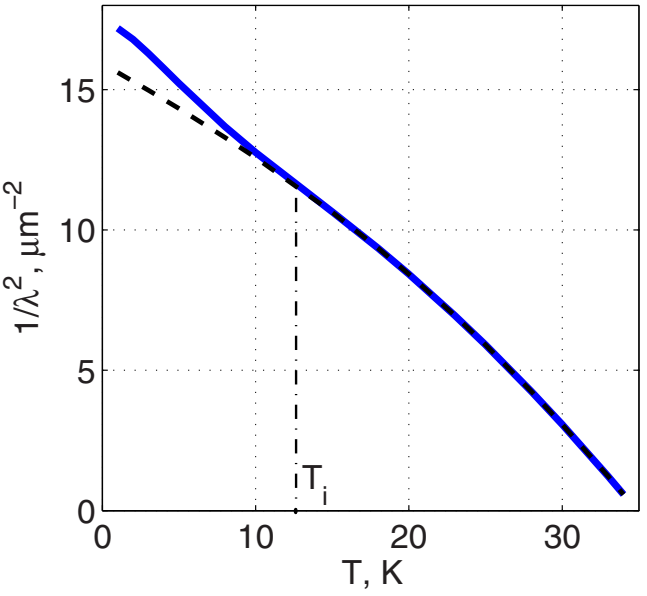


**Fig. 6.** Temperature dependence of the inverse square of the magnetic penetration depth at $x = 0.17$. The model parameters are as follows (in eV): $\tau = 0.225$, $J = 1.42$, $I = 0.056$ and $t = 0.12$. The magnitudes of $J$ and $I$ were chosen in such a way as to conform the curve $\lambda^{-2}(T)$ with the experimental one for $La_{1.83}Sr_{0.17}CuO_4$ [76,79,80]. Vertical dash-dotted line indicates location of the inflection point $T_i \approx 13$ K. Dashed line at $T < T_i$ is extrapolation of the function $\lambda^{-2}(T)$ from the right side of $T_i$.

It can be seen from Figure 4 that in the low temperature region all the curves show linear behavior down to the lowest considered temperature $T = 2$ K. Such a behavior is usually regarded as a manifestation of the $d$-wave symmetry of the SC order parameter [73]. For $x$ corresponding to the overdoped cuprates ($x \gtrsim 0.16$) the functions $\lambda^{-2}(T)$ in overall are slightly convex as it is in the most experiments on cuprate superconductors [74,75,79].

At doping levels $x$ close to optimal in the temperature dependence of $\lambda^{-2}$ a remarkable feature appears: the inflection point where the function $\lambda^{-2}(T)$ changes its curvature (see also Fig. 6). At lower temperatures the shape of $\lambda^{-2}(T)$ is concave, wile at elevated temperatures the function becomes convex. In reference [76] to explain such an unusual behavior of the superfluid density observed in $La_{1.83}Sr_{0.17}CuO_4$ the existence of two SC gaps with different $d$- and $s$-symmetry was suggested. As it follows from our study, the inflection point in $La_{1.83}Sr_{0.17}CuO_4$ detected experimentally [76,80] may not be necessarily related to the presence of two SC gaps, but instead can be regarded as a manifestation of the spin-polaron nature of quasiparticles in cuprate superconductors.

It should also be noted that occurrence of the inflection point in the temperature dependence of $\lambda^{-2}$ is not restricted by only LSCO superconductors [76,80], it was also detected in $YBa_2Cu_3O_{7-\delta}$ [74,77] and $Bi_{2.15}Sr_{1.85}CaCu_2O_{8+\delta}$ [78].

In the underdoped case, related to doping level $x$ less than optimal ($x_{opt} = 0.16$), the concave shape of $\lambda^{-2}(T)$ visible on the entire temperature range (the curve with $x = 0.10$ in Fig. 4) seems to be inconsistent with the experimental results. This discrepancy is most likely because we did not take into account the pseudogap behavior exhibited by underdoped cuprates. The PG we believe arises due to the spin and charge fluctuations (SCF) that considerably modify the spectral intensity on the Fermi contour. The present theory is essentially a mean-field theory and does not take into account the SCF and hence the PG. No doubt that temperature dependent modifications of the quasiparticle spectral density due to the PG behavior will lead to the changes in temperature dependence of the superfluid density in the underdoped ($x < x_{opt}$) cuprates. However since the PG is absent for dopings $x > x_{opt}$ we are sure that in optimally doped and overdoped cuprates the results delivered in this paper will remain unchanged.

## 9 Conclusion

In conclusion we dwell on the main points of the study we carried out.

First, a novel approach for calculating the magnetic penetration depth is developed. The main idea of this approach is to derive an analytical expression for the current density $\vec{j}(\vec{q} = 0)$ rather then for the response function. This allows us not to expand the current density in powers of vector potential $\vec{A}_{\vec{q}=0}$ (taken in the long-wavelength limit) and hence not to be limited to small values of $\vec{A}_{\vec{q}=0}$. The magnetic penetration depth then is found numerically as the ratio of $\vec{j}(\vec{q} = 0)$ to $\vec{A}_{\vec{q}=0}$ at reasonably chosen small values of the vector potential. Such an approach turns out to be rather efficient especially for the multiband system for which $k$-dependence of the

quasiparticle spectrum is not known analytically and have to be computed only numerically. Particulary, within the proposed approach there is no need to carry out cumbersome calculations related to extracting the paramagnetic and diamagnetic parts of the supercurrent density.

The developed approach was used to calculate the temperature and concentration dependence of the magnetic penetration depth in the hole-doped cuprate superconductors within the framework of the spin-polaron concept [8,51]. It is important that the obtained equation (56) for the supercurrent density takes rigorously into account the strong coupling ($J$) between a localized spin on the copper ion and a hole residing on the four nearest oxygen ions. It turns out that almost entire contribution to the supercurrent density $\vec{j}(\vec{q}=0)$ is due to the third term in equation (56) which is proportional to $J$. This means that it is hoppings of the spin-polaron quasiparticles rather than hoppings of bare holes are responsible for the supercurrent to occur.

Obtained temperature dependencies of $\lambda^{-2}$ demonstrate monotonic decrease. Both the magnitudes of $\lambda^{-2}(T=0)$ and superconducting critical temperature $T_c$, at which $\lambda$ diverges, are well consistent with the experimental results. For overdoped system we obtained convex shape of the function $\lambda^{-2}(T)$ which is observed in most cuprate superconductors. Moving down to optimal dopings the inflection point in the temperature dependence of $\lambda^{-2}$ appears. We argue that this inflection point, well known for instance in the slightly overdoped LSCO [76] and commonly believed to occur due to two SC gaps, can in fact serve as a manifestation of the spin-polaron nature of quasiparticles in cuprates.

At low dopings ($x<0.16$), the obtained concave shape of the function $\lambda^{-2}(T)$ on the entire temperature range is, as we think, due to the spin-polaron character of the quasiparticles as well. Such a behavior seems not to be in full consistency with available experimental data. We mainly relate this discrepancy to the, inherent to underdoped cuprates, pseudogap behavior which we did not take into account in the present formulation of our approach. Besides, some other processes, that were not considered but are going to be, may also improve our results concerning low doping regime. Among them are (1) Coulomb interaction between holes both on site and intersite, and (2) impurity scattering which is assumed to be responsible for the convex shape of $\lambda^{-2}$ as a function of temperature [72].

We would like to thank V.V. Val'kov, A.F. Barabanov, and M.M. Korovushkin for helpful and stimulating discussions. The work was financially supported by the Russian Foundation for Basic Research (RFBR) (project no. 18-02-00837) and by the program of the Presidium of the Russian Academy of Sciences No. 12 "Fundamental problems of high-temperature superconductivity". The work of K. K. K. was supported by the grant of the President of the Russian Federation (project MK-1398.2017.2) and the RFBR and partly by the Government of Krasnoyarsk Region and the Krasnoyarsk Region Science and Technology Support Fund (project no. 18-42-243002).

## Author contribution statement

This work was proposed by D.M.D. Both authors, D.M.D. and K.K.K., contributed to the analytical and numerical calculations, and were involved in the preparation of the manuscript.

## Appendix

In the Appendix we will present particular calculations of the energy matrix elements: $D_{13}(k)$, $D_{23}(k)$, $D_{33}(k)$, and $D_{36}(k)$, for which approximations were used.

The equations of motion for two first basis operators $a_{k\uparrow}$ and $b_{k\uparrow}$ are

$$\left[a_{k\uparrow},\hat{\mathscr{H}}\right]=\xi_{kx}a_{k\uparrow}+\Gamma_k b_{k\uparrow}+J\nu_{kx}L_{k\uparrow}, \tag{A.1}$$

$$\left[b_{k\uparrow},\hat{\mathscr{H}}\right]=\xi_{ky}b_{k\uparrow}+\Gamma_k a_{k\uparrow}+J\nu_{ky}L_{k\uparrow}. \tag{A.2}$$

Using equation (A.1) and the definition of matrix elements (19) we find for the element $D_{13}(k)$ an expression:

$$D_{13}(k)=(\xi_{kx}\nu_{kx}+\Gamma_k\nu_{ky})\frac{1}{N}\sum_f\langle\tilde{S}_f^{\uparrow\uparrow}\rangle+J\nu_{kx}K_k, \tag{A.3}$$

where

$$K_k=\langle\{L_{k\uparrow},L_{k\uparrow}^{+}\}\rangle. \tag{A.4}$$

Since the system is in SU(2)-invariant spin-liquid phase we have $\langle\tilde{S}_f^{\uparrow\uparrow}\rangle\equiv\langle S_f^z\rangle=0$. Thus, from (A.3) follows the expression for $D_{13}(k)$ given in (24). Similarly, we find expression for matrix element $D_{23}(k)$ using equation of motion (A.2).

Calculating anticommutator in (A.4) we obtain:

$$K_k=\sum_q\langle\left(\tilde{S}_{k-q}\tilde{S}_{q-k}\right)_{\uparrow\uparrow}\rangle\nu_q^2 + \sum_{qp\alpha\beta}\langle u_{p\beta}^{+}u_{q\alpha}[\tilde{S}_{p-k}^{\beta\uparrow},\tilde{S}_{k-q}^{\uparrow\alpha}]\rangle, \tag{A.5}$$

where $\nu_q^2=\nu_{qx}^2+\nu_{qy}^2$. The second term in the right-hand side of (A.5) contains fermi-operators and hence, according to the low-density approximation discussed in the Section 4 can be neglected. Doing Fourier transform in the first term and taking into account definition of $\nu_{kx(y)}$ (see (11)) yields:

$$K_k=\frac{3}{4}-\frac{C_1}{2}\left(\cos(k_x-2\alpha_x)+\cos(k_y)\right), \tag{A.6}$$

where $C_1=\langle\left(\tilde{S}_f\tilde{S}_{f+2\delta}\right)_{\uparrow\uparrow}\rangle=\langle\vec{S}_f\vec{S}_{f+2\delta}\rangle$ in agreement with the definition of spin correlators (5). Thus, (A.6) corresponds to (25).

To derive matrix elements $D_{33}(k)$ and $D_{36}(k)$ let us first write down the equation of motion for $L_{k\uparrow}$:

$$\left[L_{k\uparrow},\hat{\mathscr{H}}\right]=\sum_{q\alpha}\tilde{S}^{\uparrow\alpha}_{k-q}\left[(\xi_{kx}\nu_{kx}+\Gamma_q\nu_{qy})a_{k\uparrow}\right.$$
$$\left.+(\xi_{ky}\nu_{ky}+\Gamma_q\nu_{qx})b_{k\uparrow}\right]+J\sum_{qp\alpha}\nu_q^2\left(\tilde{S}_{k-q}\tilde{S}_{q-p}\right)_{\uparrow\alpha}$$
$$\times u_{p\alpha}+J\sum_{qpk'\alpha\beta\gamma}[\tilde{S}^{\uparrow\alpha}_{k-q},\tilde{S}^{\beta\gamma}_{k'-p}]u^{+}_{k'\beta}u_{p\gamma}u_{q\alpha}$$
$$+\frac{i}{N}\sum_{fmq\alpha}I_{fm}e^{-im(k-q)}\vec{\sigma}_{\uparrow\alpha}\left(\vec{S}_f\times\vec{S}_m\right)u_{q\alpha},\quad(A.7)$$

where, for convenience, we consider exchange interaction between arbitrary sites $f$ and $m$, not restricted by nearest neighbors approximation as in the main text. Using this equation we can express the element $D_{33}(k)$ as a sum of five terms:

$$D_{33}(k)=\sum_{qp\alpha\beta}(\xi_{qx}\nu_{qx}+\Gamma_q\nu_{qy})\langle\{\tilde{S}^{\uparrow\alpha}_{k-q}a_{q\alpha},u^{+}_{p\beta}\tilde{S}^{\beta\uparrow}_{p-k}\}\rangle$$
$$+\sum_{qp\alpha\beta}(\xi_{qy}\nu_{qy}+\Gamma_q\nu_{qx})\langle\{\tilde{S}^{\uparrow\alpha}_{k-q}b_{q\alpha},u^{+}_{p\beta}\tilde{S}^{\beta\uparrow}_{p-k}\}\rangle$$
$$+J\sum_{qpp'\alpha\beta}\nu_q^2\langle\{\left(\tilde{S}_{k-q}\tilde{S}_{q-p}\right)_{\uparrow\alpha}u_{p\alpha},u^{+}_{p'\beta}\tilde{S}^{\beta\uparrow}_{p'-k}\}\rangle$$
$$+J\sum_{qpk'p'\alpha\beta\gamma\beta'}\langle\{[\tilde{S}^{\uparrow\alpha}_{k-q},\tilde{S}^{\beta\gamma}_{k'-p}]u^{+}_{k'\beta}u_{p\gamma}u_{q\alpha},u^{+}_{p'\beta'}\tilde{S}^{\beta'\uparrow}_{p'-k}\}\rangle$$
$$+\frac{i}{N}\sum_{qpfm\alpha\beta}I_{fm}e^{-im(k-q)}$$
$$\times\langle\{\vec{\sigma}_{\uparrow\alpha}\left(\vec{S}_f\times\vec{S}_m\right)u_{q\alpha},u^{+}_{p\beta}\tilde{S}^{\beta\uparrow}_{p-k}\}\rangle.\quad(A.8)$$

Each of these five terms includes an anticommutator of the form $[S_1f_1,f_2S_2]$, where $S_{1(2)}$ is a Bose-like (spin) operator and $f_{1(2)}$ is a Fermi-like operator. Since the anticommutator can be expressed as

$$\{S_1f_1,f_2S_2\}=f_1f_2[S_1,S_2]+\{f_1,f_2\}S_1S_2,\quad(A.9)$$

each of the five terms in (A.8) can be divided into two components. The first component, corresponding to the first term in (A.9), contains fermi operators and, according to the adopted low-density approximation, can be neglected. The second component, corresponding to the second term in (A.9), after calculating the anticommutator either contains Fermi operators (as the fourth sum in (A.8)) or does not contain. Keeping only these last terms (with no Fermi operators) we obtain:

$$D_{33}(k)=J\sum_{qp}\nu_q^2\nu_p^2\langle\left(\tilde{S}_{k-q}\tilde{S}_{q-p}\tilde{S}_{p-k}\right)_{\uparrow\uparrow}\rangle$$
$$+\sum_q(\xi_{qx}\nu_{qx}^2+\xi_{qy}\nu_{qy}^2+2\Gamma_q\nu_{qx}\nu_{qy})\langle\left(\tilde{S}_{k-q}\tilde{S}_{q-k}\right)_{\uparrow\uparrow}\rangle$$
$$+\frac{i}{N}\sum_{qfm\alpha}I_{fm}e^{-im(k-q)}\nu_q^2\langle\vec{\sigma}_{\uparrow\alpha}\left(\vec{S}_f\times\vec{S}_m\right)\tilde{S}^{\alpha\uparrow}_{q-k}\rangle.\quad(A.10)$$

Doing the inverse Fourier transformation for the spin operators we can express the pair spin average in (A.10) as

$$\langle\left(\tilde{S}_{k-q}\tilde{S}_{q-k}\right)_{\uparrow\uparrow}\rangle=\frac{1}{N}C_{q-k},\quad(A.11)$$

where $C_k=\sum_f e^{-ifk}C_f$ is a Fourier transform of the spin correlator (5). Similarly, for the triple spin average in (A.10) we have

$$\langle\left(\tilde{S}_{k-q}\tilde{S}_{q-p}\tilde{S}_{p-k}\right)_{\uparrow\uparrow}\rangle=\frac{1}{N^2}\left(C_{q-p}-C_{p-k}-C_{k-q}\right),\quad(A.12)$$

where it was taken into account that when all three spins are at different sites the average is zero due to SU(2)-invariance.

The condition of SU(2)-invariance and, following from it identity: $\langle S_f^+S_m^--S_f^-S_m^+\rangle\equiv 0$ $(f\neq m)$, were also used when calculating the third average in (A.10). The final result for $D_{33}(k)$ reads

$$D_{33}(k)=\frac{J}{N^2}\sum_{qp}\nu_q^2\nu_p^2\left(C_{q-p}-C_{p-k}-C_{k-q}\right)$$
$$+\frac{1}{N}\sum_q(\xi_{qx}\nu_{qx}^2+\xi_{qy}\nu_{qy}^2+2\Gamma_q\nu_{qx}\nu_{qy})C_{q-k}$$
$$+\frac{1}{N}\sum_q I_q\left(\frac{1}{N}\sum_p C_p\nu^2_{k+p-q}-C_q\right).\quad(A.13)$$

Performing inverse Fourier transform in equation (A.13) and adopting the nearest neighbor approximation for exchange integral $I_{fm}$ we come to the expression for $D_{33}(k)$ provided in the formula (24).

The only contribution to the anomalous matrix element $D_{36}=\langle\{[L_{k\uparrow},\hat{\mathscr{H}}],L_{-k\downarrow}\}\rangle$, for $d$-wave pairing, is due to the exchange interaction between localized spins. Taking into account only this interaction in the equation of motion (A.7) we obtain

$$D_{36}(k)=\frac{i}{N}\sum_{qpfm\alpha\beta}I_{fm}e^{-im(k-q)}$$
$$\times\langle\{\vec{\sigma}_{\uparrow\alpha}\left(\vec{S}_f\times\vec{S}_m\right)u_{q\alpha},\tilde{S}^{\downarrow\beta}_{-k-p}u_{p\beta}\}\rangle.\quad(A.14)$$

In calculating the anomalous average in the right hand side of (A.14) the low-density approximation, used above for normal averages, not necessary. Instead our goal now is to express the result of anticommutation in the anomalous average via the two basis destruction operators. Straightforward calculation of (A.14) gives

$$D_{36}(k)=-\frac{1}{N}\sum_{qpq'}I_{q'}\left[3\langle\left(\vec{S}_{-q'}\vec{S}_{-q-p+q'}\right)u_{q\downarrow}u_{p\uparrow}\rangle\right.$$
$$+\langle\left(\tilde{S}_{-q'}u_p\right)_{\downarrow}\left(\tilde{S}_{-q-p+q'}u_q\right)_{\uparrow}\rangle$$
$$-3\langle\left(\vec{S}_{-q'-k-p}\vec{S}_{k-q+q'}\right)u_{q\downarrow}u_{p\uparrow}\rangle$$
$$\left.+\langle\left(\tilde{S}_{-q'-k-p}u_q\right)_{\uparrow}\left(\tilde{S}_{k-q+q'}u_p\right)_{\downarrow}\rangle\right].\quad(A.15)$$

The first two terms in (A.15) do not contribute to the $d$-wave pairing and therefore can be discarded. The last term due to the SU(2)-invariance (specifically invariance of the system under rotation by angle $\pi$) can be expressed as

$$\begin{aligned}\langle\left(\tilde{S}_{-q'-k-p}u_q\right)_\uparrow\left(\tilde{S}_{k-q+q'}u_p\right)_\downarrow\rangle \\ = 2\langle\left(\vec{S}_{-q'-k-p}\vec{S}_{k-q+q'}\right)u_{q\downarrow}u_{p\uparrow}\rangle \\ -\langle\left(\tilde{S}_{-q'-k-p}u_p\right)_\uparrow\left(\tilde{S}_{k-q+q'}u_q\right)_\downarrow\rangle. \quad \text{(A.16)}\end{aligned}$$

This identity, after summation over the quasimomenta $q$ and $p$, allows to express the anomalous element $D_{36}(k)$ in terms of the basis operators $L_{k\sigma}$:

$$\begin{aligned}D_{36}(k) = \frac{1}{N}\sum_{q'} I_{q'}\langle L_{-q'-k,\uparrow}L_{k+q',\downarrow}\rangle \\ +\frac{1}{N}\sum_{qpq'} I_{q'}\langle\left(\vec{S}_{-q'-k-p}\vec{S}_{k-q+q'}\right)u_{q\downarrow}u_{p\uparrow}\rangle. \quad \text{(A.17)}\end{aligned}$$

Decoupling the second term in equation (A.17) we arrive at expression (36).

## References


1. P.W. Anderson, Science **235**, 1196 (1987)
2. L.A. Maksimov, A.F. Barabanov, R.O. Kuzian, Phys. Lett. A **232**, 286 (1997)
3. A.F. Barabanov, O.V. Urazaev, A.A. Kovalev, L.A. Maksimov, JETP Lett. **68**, 412 (1998)
4. R.O. Kuzian, A.F. Barabanov, L.B. Litinskii, Phys. Lett. A **273**, 345 (2000)
5. A. Ramšak, P. Prelovšek, Phys. Rev. B **42**, 10415 (1990)
6. V.V. Val'kov, M.M. Korovushkin, A.F. Barabanov, JETP Lett. **88**, 370 (2008)
7. A.F. Barabanov, L.A. Maksimov, L.E. Zhukov, Physica C **212**, 375 (1993)
8. A.F. Barabanov, V.M. Berezovskii, E. Zasinas, L.A. Maksimov, JETP **83**, 819 (1996)
9. A.F. Barabanov, R.O. Kuzian, L.A. Maksimov, Phys. Rev. B **55**, 4015 (1997)
10. R.O. Kuzian, R. Hayn, A.F. Barabanov, L.A. Maksimov, Phys. Rev. B **58**, 6194 (1998)
11. A.F. Barabanov, L.A. Maksimov, G.V. Uimin, JETP Lett. **47**, 622 (1988)
12. J. Zaanen, A.M. Oleś, Phys. Rev. B **37**, 9423 (1988)
13. V.J. Emery, G. Reiter, Phys. Rev. B **38**, 4547 (1988)
14. P. Prelovšek, Phys. Lett. A **126**, 287 (1988)
15. E.B. Stechel, D.R. Jennison, Phys. Rev. B **38**, 4632 (1988)
16. A.F. Barabanov, L.A. Maksimov, G.V. Uimin, Sov. Phys. JETP **69**, 371 (1989)
17. H. Matsukawa, H. Fukuyama, J. Phys. Soc. Jpn. **58**, 2845 (1989)
18. A. Ramšak, P. Prelovšek, Phys. Rev. B **40**, 2239 (1989)
19. V.J. Emery, Phys. Rev. Lett. **58**, 2794 (1987)
20. C.M. Varma, S. Schmitt-Rink, E. Abrahams, Solid State Commun. **62**, 681 (1987)
21. J.E. Hirsch, Phys. Rev. Lett. **59**, 228 (1987)
22. Yu.B. Gaididei, V.M. Loktev, Phys. Status Solidi B **147**, 307 (1988)
23. S.G. Ovchinnikov, I.S. Sandalov, Physica C **161**, 607 (1989)
24. J.C. Hubbard, Proc. R. Soc. A **276**, 238 (1963)
25. K.A. Chao, J. Spalek, A.M. Oles, J. Phys. C: Solid State Phys. **10**, L271 (1977)
26. R. Zwanzig, Phys. Rev. **124**, 983 (1961)
27. H. Mori, Prog. Theor. Phys. **33**, 423 (1965)
28. L.M. Roth, Phys. Rev. Lett. **20**, 1431 (1968)
29. L.M. Roth, Phys. Rev. **184**, 451 (1969)
30. D.J. Rowe, Rev. Mod. Phys. **40**, 153 (1968)
31. Y.A. Tserkovnikov, Teor. Mat. Fiz. **49**, 219 (1981)
32. Y.A. Tserkovnikov, Theor. Math. Phys. **52**, 712 (1982)
33. N.M. Plakida, *High-Temperature Cuprate Superconductors* (Springer, Berlin, 2010)
34. W. Nolting, A.M. Oles, J. Phys. C: Solid St. Phys. **13**, 2295 (1980)
35. F. Mancini, A. Avella, Adv. Phys. **53**, 537 (2004)
36. A. Avella, F. Mancini, in *Theoretical Methods for Strongly Correlated Systems*, Springer Series in Solid-State Sciences (Springer-Verlag, Berlin, 2012), Vol. 171, p. 103
37. A. Avella, Eur. Phys. J. B **87**, 45 (2014)
38. A. Avella, Adv. Cond. Matt. Phys. **2014**, 515698 (2014)
39. J. Kondo, K. Yamaji, Prog. Theor. Phys. **47**, 807 (1972)
40. M. Takahashi, Phys. Rev. B **40**, 2494 (1989)
41. H. Shimahara, S. Takada, J. Phys. Soc. Jpn. **60**, 2394 (1991)
42. V.V. Val'kov, D.M. Dzebisashvili, JETP **100**, 608 (2005)
43. M.M. Korshunov, S.G. Ovchinnikov, Eur. Phys. J. B **57**, 271 (2007)
44. A.F. Barabanov, A.V. Mikheenkov, A.V. Shvartsberg, Theor. Math. Phys. **168**, 1192 (2011)
45. A. Sherman, Phys. Lett. A **309**, 482 (2003)
46. F.C. Zhang, T.M. Rice, Phys. Rev. B **37**, 3759 (1988)
47. A. Damascelli, Z. Hussain, Z.-X. Shen, Rev. Mod. Phys. **75**, 473 (2003)
48. A.F. Barabanov, R.O. Kuzian, L.A. Maksimov, J. Phys: Condens. Matter **3**, 9129 (1991)
49. O.A. Starykh, O.F. de Alcantara Bonfim, G.F. Reiter, Phys. Rev. B **52**, 12534 (1995)
50. A.F. Barabanov, E. Zasinas, O.V. Urazaev, L.A. Maksimov, JETP Lett. **66**, 182 (1997)
51. A.F. Barabanov, A.A. Kovalev, O.V. Urazaev, A.M. Belemuk, R. Hayn, JETP **92**, 677 (2001)
52. R.O. Kuzian, R. Hayn, A.F. Barabanov, Phys. Rev. B **68**, 195106 (2003)
53. T. Yoshida, X.J. Zhou, D.H. Lu, S. Komiya, Y. Ando, H. Eisaki, T. Kakeshita, S. Uchida, Z. Hussain, Z.-X. Shen, A. Fujimori, J. Phys: Condens. Matter **19**, 125209 (2007)
54. D.M. Dzebisashvili, V.V. Val'kov, A.F. Barabanov, JETP Lett. **98**, 528 (2013)
55. V.V. Val'kov, D.M. Dzebisashvili, A.F. Barabanov, JETP **118**, 959 (2014)
56. V.V. Val'kov, D.M. Dzebisashvili, A.F. Barabanov, Phys. Lett. A **379**, 421 (2015)
57. V.V. Val'kov, D.M. Dzebisashvili, A.F. Barabanov, J. Low Temp. Phys. **181**, 134 (2015)
58. V.V. Val'kov, D.M. Dzebisashvili, A.F. Barabanov, J. Supercond. Nov. Magn. **29**, 1049 (2016)
59. V.V. Val'kov, D.M. Dzebisashvili, M.M. Korovuskin, A.F. Barabanov, JETP Lett. **103**, 385 (2016)

60. V.V. Val'kov, D.M. Dzebisashvili, M.M. Korovuskin, A.F. Barabanov, J. Magn. Magn. Mater. **440**, 123 (2017)
61. V.V. Val'kov, D.M. Dzebisashvili, M.M. Korovuskin, A.F. Barabanov, JETP **125**, 810 (2017)
62. J.R. Schriffer, *Theory of Superconductivity* (Benjamin, New York, 1964)
63. M. Tinkham, *Introduction to Superconductivity* (McGraw-Hill, New York, 1996)
64. S.B. Nam, Phys. Rev. **156**, 470 (1967)
65. D.J. Scalapino, S.R. White, S.C. Zhang, Phys. Rev. Lett. **68**, 2830 (1992)
66. S. Misawa, Phys. Rev. B **51**, 11791 (1995)
67. W.A. Atkinson, J.P. Carbotte, Phys. Rev. B **52**, 10601 (1995)
68. L. Benfatto, S. Caprara, C. Di Castro, Eur. Phys. J. B **17**, 95 (2000)
69. D.E. Sheehy, T.P. Davis, M. Franz, Phys. Rev. B **70**, 054510 (2004)
70. M.V. Eremin, I.A. Larionov, I.E. Lyubin, J. Phys: Condens. Matter **22**, 185704 (2010)
71. Z. Huang, H. Zhao, S. Feng, Phys. Rev. B **83**, 144524 (2011)
72. I. Bozovic, X. He, J. Wu, A.T. Bollinger, Nature **536**, 309 (2016)
73. W.N. Hardy, D.A. Bonn, D.C. Morgan, R. Liang, K. Zhang, Phys. Rev. Lett. **70**, 3999 (1993)
74. J.E. Sonier, J.H. Brewer, R.F. Kiefl, G.D. Morris, R.I. Miller, D.A. Bonn, J. Chakhalian, R.H. Heffner, W.N. Hardy, R. Liang, Phys. Rev. Lett. **83**, 4156 (1999)
75. C. Panagopoulos, B.D. Rainford, J.R. Cooper, W. Lo, J.L. Tallon, J.W. Loram, J. Betouras, Y.S. Wang, C.W. Chu, Phys. Rev. B **60**, 14617 (1999)
76. R. Khasanov, A. Shengelaya, A. Maisuradze, F. La Mattina, A. Bussmann-Holder, H. Keller, K.A. Muller, Phys. Rev. Lett. **98**, 057007 (2007)
77. R. Khasanov, S. Strassle, D. Di Castro, T. Masui, S. Miyasaka, S. Tajima, A. Bussmann-Holder, H. Keller, Phys. Rev. Lett. **99**, 237601 (2007)
78. W. Anukool, S. Barakat, C. Panagopoulos, J.R. Cooper, Phys. Rev. B **80**, 024516 (2009)
79. T.R. Lemberger, I. Hetel, A. Tsukada, M. Naito, Phys. Rev. B **82**, 214513 (2010)
80. B.M. Wojek, S. Weyeneth, S. Bosma, E. Pomjakushina, R. Puzniak, Phys. Rev. B **84**, 144521 (2011)
81. M.S. Hybertsen, M. Schluter, N.E. Christensen, Phys. Rev. B **39**, 9028 (1989)
82. M. Ogata, H. Fukuyama, Rep. Prog. Phys. **71**, 036501 (2008)